

Hexagonal ice transforms at high pressures and compression rates directly into "doubly metastable" ice phases.

Marion Bauer, Katrin Winkel, Daniel M. Toebebens, Erwin Mayer, Thomas Loerting; **J. Chem. Phys.** 131 (2009) 224514.

Supporting Information:

Phase analysis of the X-ray powder diffraction data by application of the Rietveld method

X-ray powder diffraction data were measured in $\Theta/2\Theta$ geometry on a Siemens D5000 diffractometer equipped with an Anton Paar low-temperature camera. The Θ/Θ arrangement of the instrument allowed keeping the sample in a horizontal position throughout the experiment. The instrument is equipped with a Goebel mirror, providing monochromatic $\text{Cu K}\alpha_1$ radiation. This setup provides high intensity, stability of peak positions, and low background, which allows for reliable identification of minor phases in small samples. The samples were prepared as described in the main text and in the caption to Figure 2. Diffractograms were measured at a temperature of ~ 80 K after peeling off the indium linings and powdering the sample in liquid nitrogen at 77 K. We have not detected any significant difference between powdered and unpowdered samples, so the sample preparation in liquid nitrogen does not affect the metastable phases. We have also learned over the years how to transfer the samples, which are stored in liquid nitrogen, to the sample holder kept at ~ 80 K without significant condensation of water vapour from humid air onto the sample. Basically, it is critical to do the transfer fast (about 5 seconds) and to evacuate the leak-tight chamber immediately to less than 100 mbar. Under these conditions condensation of water vapour onto the sample is slowed down/prevented by evaporation of liquid nitrogen still adhering to the sample. This technique has proven in the past to be capable of producing powder X-ray diffractograms, in which no hexagonal ice is detectable. In the present study in some diffractograms no condensed hexagonal ice is detectable, whereas in the worst case (of a slow transfer and high humidity in the lab) 1 – 2% of hexagonal ice condensed onto the sample. Transfer units purged with dry nitrogen gas have turned out to be counterproductive because of the longer handling times.

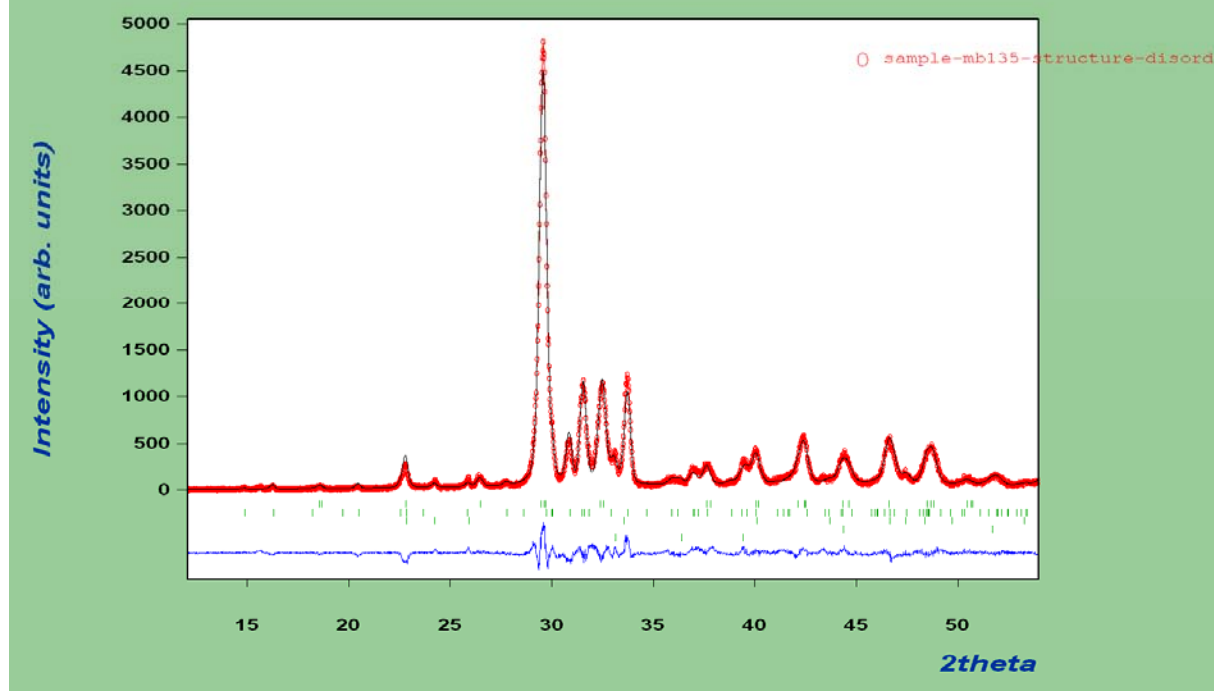
Initial phase identification was done using the published crystal structures of high pressure polymorphs with the aid of the program PowderCell⁴⁵. Subsequently, a quantitative phase analysis with the Rietveld method was performed with the program FullProf⁵⁰. Peak width and shape were described with the Thompson-Cox-Hastings-Pseudo-Voigt function and an asymmetry correction proposed by Finger et al.⁵¹. The instrumental resolution function was determined from a measurement of Cordierite KRM 106⁵² which has sufficient low-angle peaks. Parameters refined during the phase analysis were lattice parameters of each phase, intensity scale factors, 4 parameters of a polynomial background expansion, a common isotropic Debye-Waller-factor for all phases. The peak width parameters U and Y of the TCH-PSV peak shape were refined individually for each phase with sufficiently high fraction. This accounts for eventual peak broadening due to size or strain effects. The resulting additional broadening parameters ΔU and ΔY are reported below. No further interpretation of the broadening was attempted. All estimated standard deviations given below have to be multiplied with the correction factor of Bézar⁵³ to derive reliable standard uncertainties.

The atomic positions used for the calculation of the intensities of the Bragg reflections were taken from literature^{26,30}. However, the pressure and temperature conditions here are quite different from those of the structures in literature. We therefore re-refined the structures of ices II and IX, since samples of close to 100 % purity were available. This increased the quality of the fit considerably. However, the quality of these structural data is not sufficient for publication. Only the position of the water molecules was refined. Orientation and intermolecular distances and angles were kept fixed. In particular, the atomic positions as provided in the literature were used as fixed parameters for ice Ih and ice V. In case of ice II the literature positions^{31(Kamb 1971),54}, but not the orientations, of the water molecules were refined in sample MB142. These atomic positions were used as fixed parameters in the analyses of the other samples. The structures of Ice III and Ice IX are very similar^{28(Whalley 1968),31(McFarlan 1936)}. In the initial analysis the corresponding phase was identified as Ice III. Ice III is characterized by disorder resulting in 6 hydrogen positions with 50 % occupation. Ice IX is the ordered variant, with 3 fully occupied hydrogen positions. The respective phase observed in these samples has lattice parameters *a* and *c* that are very similar to each other. This is characteristic for form IX. We used the atomic positions of Ice III³⁰ as starting values, and refined the position (but not the orientation) of the water molecules from sample MB60. In all 3 samples containing this form the distribution of the hydrogen atoms over the positions was refined (D3, D4, D8 vs. D5, D6, D7). In all samples a complete ordering resulted from the refinement, with D5, D6, D7 fully occupied and D3, D4, D8 unoccupied. This is again in agreement with the existence of form IX instead of form III at ~ 80 K, as expected^{28(Whalley 1968),55}. The resulting model of Ice IX was used for the final quantitative analysis of the respective samples.

Significant preferred orientation was found in one case only, the Ice V fraction of sample MB135. Even there the level of preferred orientation is low. If it is not corrected the fit becomes significantly worse, but the results of the quantitative phase analysis do not change significantly.

Detailed results of the phase analyses for the diffractograms shown in Fig. 3 are given in the following (Supp.-Figs. 1 – 4):

Ice IX + V + Ih; MB135



Supporting-Figure 1. Observed (red) and calculated (black) intensities and remaining difference (blue) for the diffractogram of the sample compressed at 2000 MPa/min. Observed phases are Ice IX (upper row of tick marks), Ice V (2nd row of tick marks), and Ice Ih (3rd row of tick marks). Peaks resulting from the sample holder and indium are marked in the 4th and 5th row of tick marks, respectively.

Sample:	MB135
Rate of compression:	2000 MPa/min
Rwp, Rexp, Chi2:	13.0 %, 7.0 %, 3.48
Bérar factor:	3.3
No. of contributing reflections:	141 total, 42 effective
No. of totally refined parameters:	28
No. of intensity-dependent parameters:	7

Observed phases

Ice IX

Fraction: 65.2(11) %
 Unit cell: $a = 6.7228(3) \text{ \AA}$, $c = 6.7823(7) \text{ \AA}$
 Peak broadening parameters: $\Delta U = 0.65(4)$, $\Delta Y = 0.100(4)$
 Preferred orientation: none observed

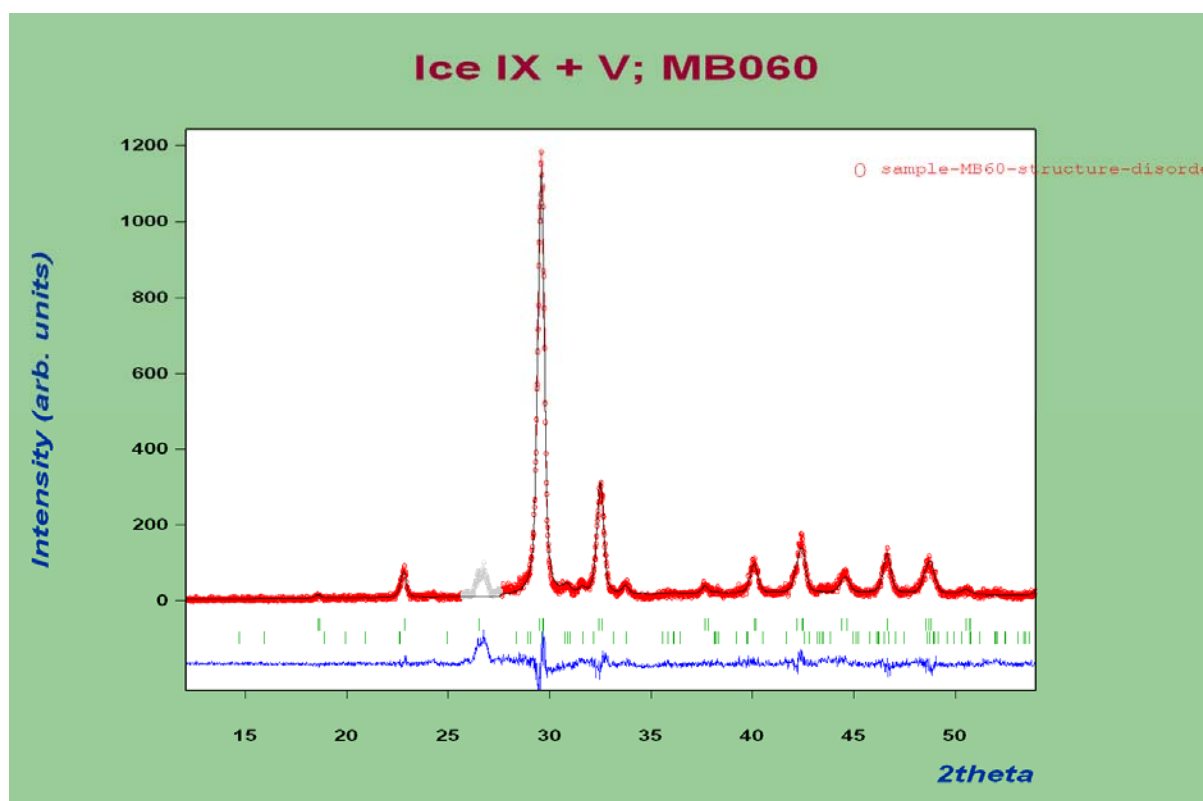
Ice V

Fraction: 33.3(6) %
 Unit cell: $a = 9.1633(5) \text{ \AA}$, $b = 7.5125(9) \text{ \AA}$, $c = 10.2951(10) \text{ \AA}$,
 $\beta = 109.14(1)^\circ$
 Peak broadening parameters: $\Delta U = 0.89(7)$, $\Delta Y = 0.000(2)$
 Preferred orientation: parallel [001], March-Dollase factor $G = 1.13(1)$

Ice Ih

Fraction: 1.5(1) %
 Unit cell: $a = 4.492(2) \text{ \AA}$, $c = 7.332(3) \text{ \AA}$
 Peak broadening parameters: as for Ice IX
 Preferred orientation: none observed

Impurities: Indium, sample holder (Cu/Ni)



Supporting-Figure 2. Observed (red) and calculated (black) intensities and remaining difference (blue) for the diffractogram of the sample compressed at 100 MPa/min. Observed phases are Ice IX (upper row of tick marks) and Ice V (lower row of tick marks).

Sample:	MB60
Rate of compression:	100 MPa/min
Rwp, Rexp, Chi2:	19.8 %, 15.5 %, 1.65
Béjar factor:	2.5
No. of contributing reflections:	120 total, 27 effective
No. of totally refined parameters:	19
No. of intensity-dependent parameters:	6

Observed phases

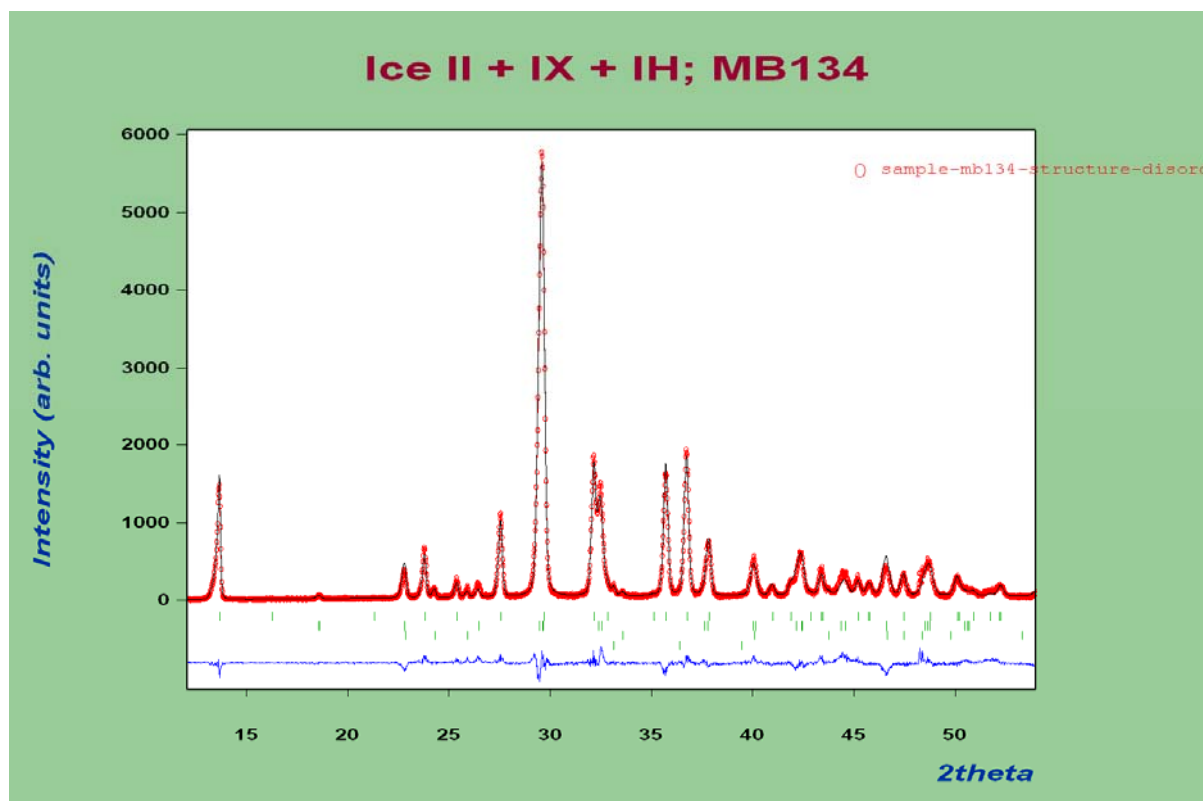
Ice IX

Fraction:	95.4(25) %
Unit cell:	$a = 6.7198(4) \text{ \AA}$, $c = 6.7722(8) \text{ \AA}$
Peak broadening parameters:	$\Delta U = 0.36(5)$, $\Delta Y = 0.121(5)$
Preferred orientation:	none observed

Ice V

Fraction:	4.6(3) %
Unit cell:	$a = 9.104(6) \text{ \AA}$, $b = 7.855(9) \text{ \AA}$, $c = 10.062(9) \text{ \AA}$, $\beta = 111.16(7)^\circ$
Peak broadening parameters:	as for Ice IX
Preferred orientation:	none observed

Impurities: One broad unaccounted peak at 26.79° , which was excluded from the refinement.



Supporting-Figure 3. Observed (red) and calculated (black) intensities and remaining difference (blue) for the diffractogram of the sample released with 5 MPa/min. Observed phases are Ice II (upper row of tick marks), Ice IX (2nd row of tick marks), and Ice Ih (3rd row of tick marks). Peaks resulting from indium are marked in the 4th row of tick marks.

Sample:	MB134
Rate of compression:	5 MPa/min
Rwp, Rexp, Chi2:	13.1 %, 6.7 %, 3.89
Bérrar factor:	4.0
No. of contributing reflections:	95 total, 35 effective
No. of totally refined parameters :	23
No. of intensity-dependent parameters:	5

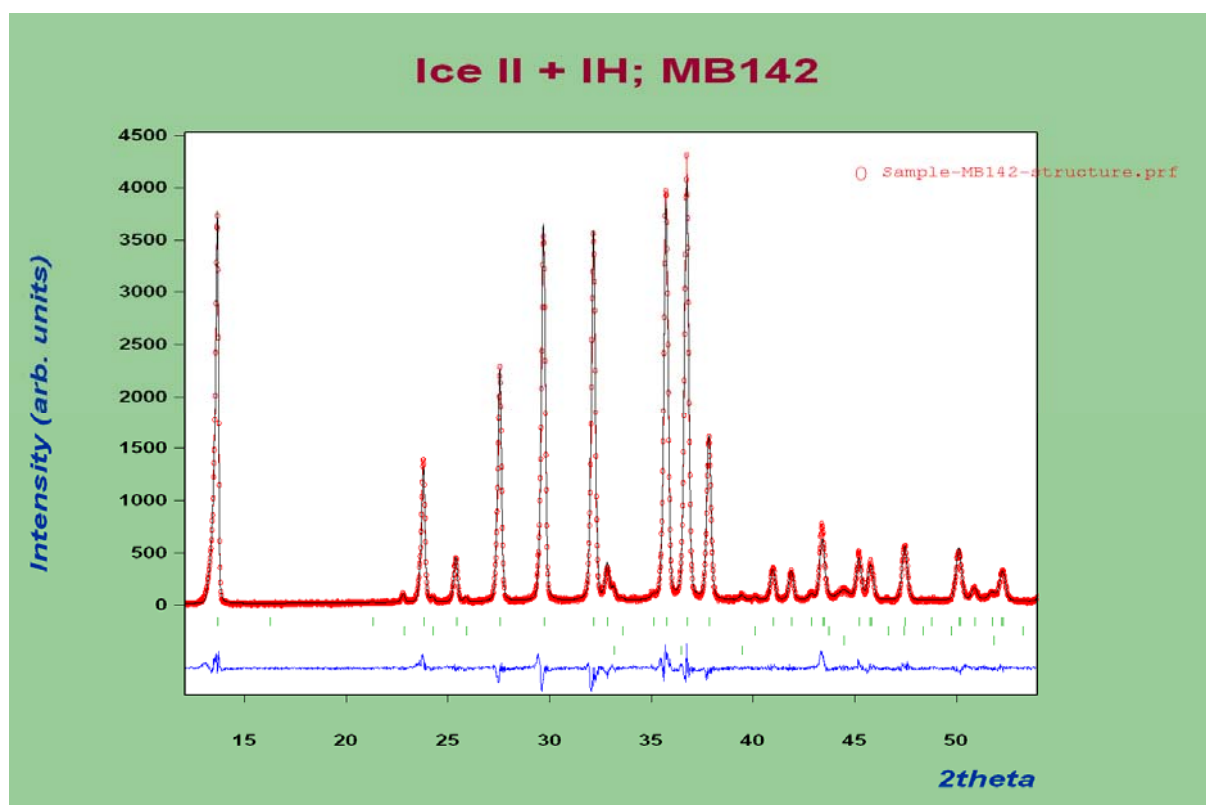
Observed phases

Ice II
 Fraction: 49.5(17) %
 Unit cell: $a = 12.9270(2) \text{ \AA}$, $c = 6.2382(2) \text{ \AA}$
 Peak broadening parameters: $\Delta U = 0.18(1)$, $\Delta Y = 0.003(2)$
 Preferred orientation: none observed

Ice IX
 Fraction: 48.6(17) %
 Unit cell: $a = 6.7290(3) \text{ \AA}$, $c = 6.7770(5) \text{ \AA}$
 Peak broadening parameters: $\Delta U = 0.41(3)$, $\Delta Y = 0.023(3)$
 Preferred orientation: none observed

Ice Ih
 Fraction: 1.9(1) %
 Unit cell: $a = 4.4915(7) \text{ \AA}$, $c = 7.3176(12) \text{ \AA}$
 Peak broadening parameters: as for Ice II
 Preferred orientation: none observed

Impurities: Indium



Supporting-Figure 4. Observed (red) and calculated (black) intensities and remaining difference (blue) for the diffractogram of the sample compressed at 2 MPa/min. Observed phases are Ice II (upper row of tick marks) and Ice Ih (2nd row of tick marks). Peaks resulting from the holder and indium are marked in the 3rd and 4th row of tick marks, respectively.

Sample:	MB142
Rate of compression:	2 MPa/min
Rwp, Rexp, Chi2:	13.5 %, 7.0 %, 3.73
Bérar factor:	3.3
No. of contributing reflections:	141 total, 42 effective
No. of totally refined parameters:	28
No. of intensity-dependent parameters:	7

Observed phases

Ice II
 Fraction: 99.2(9) %
 Unit cell: $a = 12.9251(1) \text{ \AA}$, $c = 6.2343(1) \text{ \AA}$
 Peak broadening parameters: $\Delta U = 0.146(3)$, $\Delta Y = 0.000(2)$
 Preferred orientation: none observed

Ice Ih
 Fraction: 0.8(1) %
 Unit cell: $a = 4.4917(6) \text{ \AA}$, $c = 7.326(2) \text{ \AA}$
 Peak broadening parameters: as for Ice II
 Preferred orientation: none observed

Impurities: Indium, sample holder (Cu/Ni)

Supporting References:

- (50) Rodríguez-Carvajal, J. FullProf.2k; 4.30 ed.; LLB JRC, 2008.
- (51) Finger, L. W.; Cox, D. E.; Jephcoat, A. P. *J. Appl. Crystallogr.* **1994**, *27*, 892.
- (52) Peplinski, B.; Mueller, R.; Wenzel, J.; Sojref, R.; Schultze, D. *Materials Science Forum* **1999**, *321-324*, 150.
- (53) Berar, J.-F.; Lelann, P. *J. Appl. Crystallogr.* **1991**, *24*, 1.
- (54) Finch, E. D.; Rabideau, S. W.; Wenzel, R. G.; Nereson, N. G. *J. Chem. Phys.* **1968**, *49*, 4361.
- (55) Nishibata, K.; Whalley, E. *J. Chem. Phys.* **1974**, *60*, 3189.